

## Can Great Earthquakes Occur in the Southernmost Ryukyu Arc-Taiwan Region?

Honn Kao<sup>1</sup>

(Manuscript received 20 January 1998, in final form 14 July 1998)

### ABSTRACT

Seismogenic conditions associated with the plate interface in the southernmost Ryukyu arc-Taiwan region is studied in four different aspects. From the history of large and great earthquakes, it is inconclusive whether  $M_w \geq 8$  events have ever occurred along the plate interface, but there seems to be no doubt that at least a few earthquakes with  $M_w \geq 7.0-7.5$  have occurred in the region since the turn of this century. Earthquake focal mechanisms show the co-existence of extensional earthquakes in the vicinity of trench and within the subducted lithosphere, suggesting no patterns of a seismic cycle due to strong interface coupling. The lack of "transitional thrust" earthquakes near the lower portion of the interface further supports that the interface is not strongly coupled. The maximum  $M_w$  of an interface earthquake is estimated to be 7.6-7.7, as inferred from the geometric configuration of the interface. The average slip obliquity of interface earthquakes is  $35^\circ$  while the convergence obliquity is  $70^\circ$ . Such a pattern of slip partitioning indicates that the rheological behavior of the Ryukyu fore-arc in this region is not completely elastic, thus is unlikely to generate  $M_w > 8$  subduction earthquakes. However, there is strong evidence in focal mechanisms to indicate interactions among different tectonic stress regimes. Although such interactions may not necessarily mean a bigger earthquake, they are possible to increase the frequency of earthquake occurrence because the combined stress regime would reach the failure criteria of geological materials more effectively. Given that NE Taiwan is the most likely place that interactions among various stress regimes could take place, it is suggested the seismicity there to be closely monitored. From the seismic hazard point of view, the potential threat from frequent occurrences of  $M_w > 7$  events in the region cannot be ignored. Due to the short distances from NE Taiwan to the three largest metropolitan areas on the island, improving and strictly enforcing building code and careful planning of major industrial facilities are probably the most effective measures to prevent the potential devastation due to earthquakes.

(Key words: Great earthquakes, Seismogenic structures, Ryukyu, Taiwan)

---

<sup>1</sup>Institute of Earth Sciences, Academia Sinica, P.O. Box 1-55, Nankang, Taipei, Taiwan, ROC

## 1. INTRODUCTION

Seismicity in Taiwan is among the highest in the world. In the past 5 years (1991–1996), the Seismological Observation Center of the Central Weather Bureau, Taiwan, has reported a total of 61,781 earthquakes for the region. Among them, 527 events have  $M_L \geq 4.5$ . Meanwhile, Taiwan has one of the world's highest population densities with more than 22 million people living in an area of  $\sim 36,000$  km<sup>2</sup>. Thus, careful evaluation of potential seismic hazard for the region is not only a scientific issue but also has significant societal importance.

There is a consensus among the geoscience community that the northwestward movement of the Philippine Sea Plate (PSP) relative to the Eurasia Plate (EP) is ultimately responsible for the frequent occurrence of earthquakes in the region (Figure 1). Generally speaking, the regional tectonic framework consists three major components: the Ryukyu subduction zone to the northeast, the Luzon arc–Manila trench system to the south, and the Taiwan Collision Zone between the two (Biq, 1972; Wu, 1978; Tsai, 1986). Since nearly all the world's great ( $M \geq 8$ ) earthquakes took place in convergent plate boundaries, the unique tectonic setting in Taiwan seems particularly in favor of the occurrence of such big events.

However, the occurrence of great earthquakes requires the existence of structures capable of accumulating a large amount of seismogenic strain. Kao *et al.* (1998) studied seismicity and source parameters of earthquakes that occurred between the southern Ryukyu arc and Taiwan and delineated five major seismogenic structures. They are: the Collision Seismic Zone (CSZ) along the eastern coast and offshore, the Interface Seismic Zone (ISZ) that spans between depths of 15 and 35 km, the Lateral Collision Seismic Zone (LCSZ) located in the vicinity of ISZ, the Wadati-Benioff Seismic Zone (WBSZ) within the subducted slab, and the Okinawa Seismic Zone (OSZ) associated with the opening process of the Okinawa trough (Figure 2). These structures reflect the transition from a typical tectonic setting of subduction to collision and all are capable of generating earthquakes with  $m_b \geq 5.5$ . Do they also have the potential to generate  $M \geq 8$  events? Based on the existing data and theoretical background, how much can we address this issue?

Instead of taking the region as a whole and calculating the occurrence probability corresponding to earthquakes of a certain size (e.g., Kagan and Jackson, 1994; Nishenko and Jacob, 1990), the approach of this study is to evaluate the overall seismogenic settings and/or conditions associated with individual structures in the southernmost Ryukyu arc–Taiwan region. By analyzing seismic patterns and the relationships among different structures, we shall first focus our attention on the ISZ because, on a global scale, the plate interface has generated far more great earthquakes than any other structures. We then examine the seismic potential due to the possible interactions among different structures. Finally, we discuss the implications of our study, especially on the configuration of a seismic early-warning system, should the government decide to upgrade the current one.

## 2. CONFIGURATION OF SEISMOGENIC STRUCTURES

Delineating the configuration of seismogenic structures and their relationships with respect to the various tectonic processes is the first step toward the analysis of regional seismic

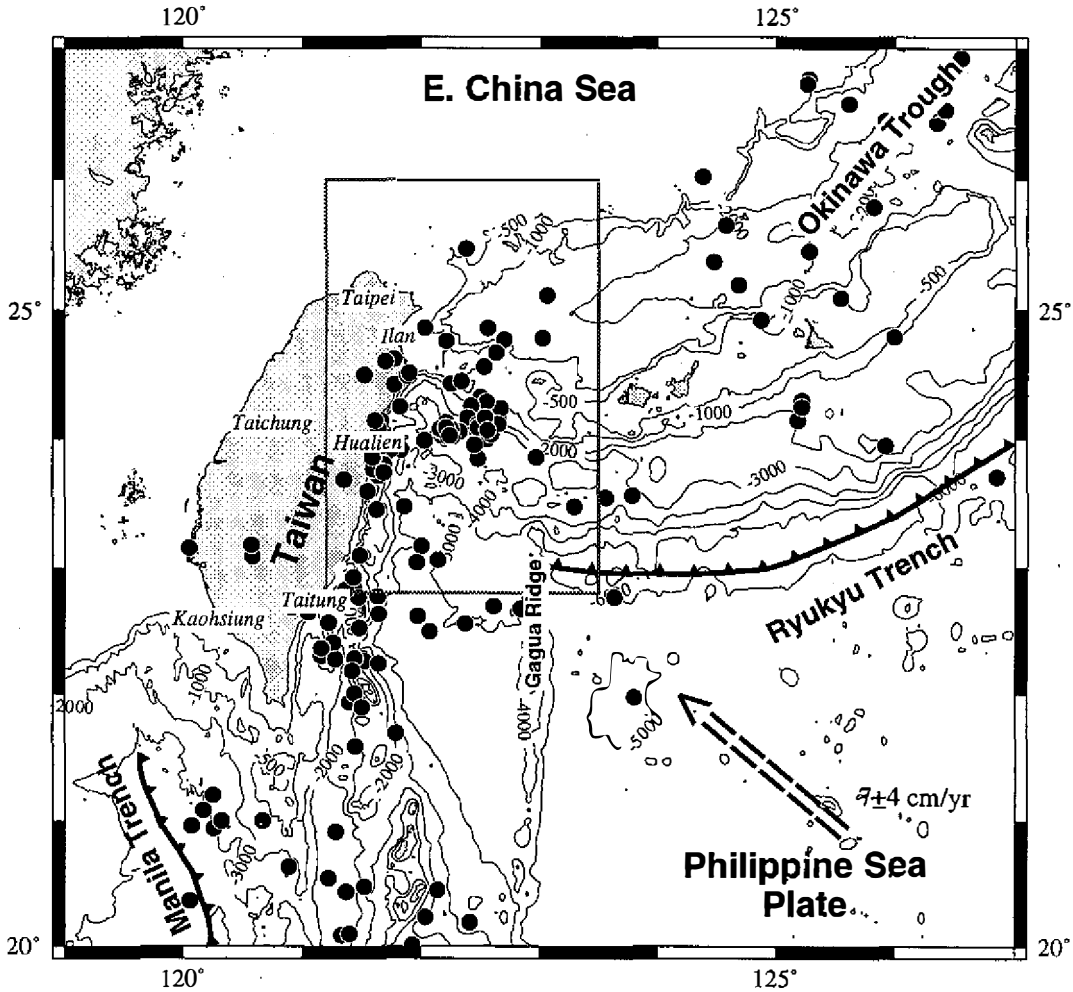


Fig. 1. Bathymetry and seismicity of  $m_b \geq 5.5$  (solid circles) between 1990 and 1996 in the southernmost Ryukyu arc-Taiwan region. The Philippine Sea plate is moving NW at  $7 \pm 4$  cm  $\text{yr}^{-1}$  relative to the Eurasia plate, resulting the Taiwan Collision Zone. Morphology of the Ryukyu trench disappears to the west of  $123^\circ\text{E}$  where it is intercepted by the Gagua Ridge. To the south of Taiwan is the Manila trench system whose bathymetric signature disappears to the north of  $\sim 21.5^\circ\text{N}$ . The smaller rectangle shows our study area.

potential. For this part, we rely on a recent study by Kao *et al.* (1998) that invert teleseismic body waveforms to determine source parameters of 62 large and moderate-sized earthquakes ( $m_b \geq 5.5$ ) occurred in the study region. Here we briefly introduce the primary results of Kao *et al.* (1998) and summarize them in Figure 2. Source parameters used in this study are listed in Table 1.

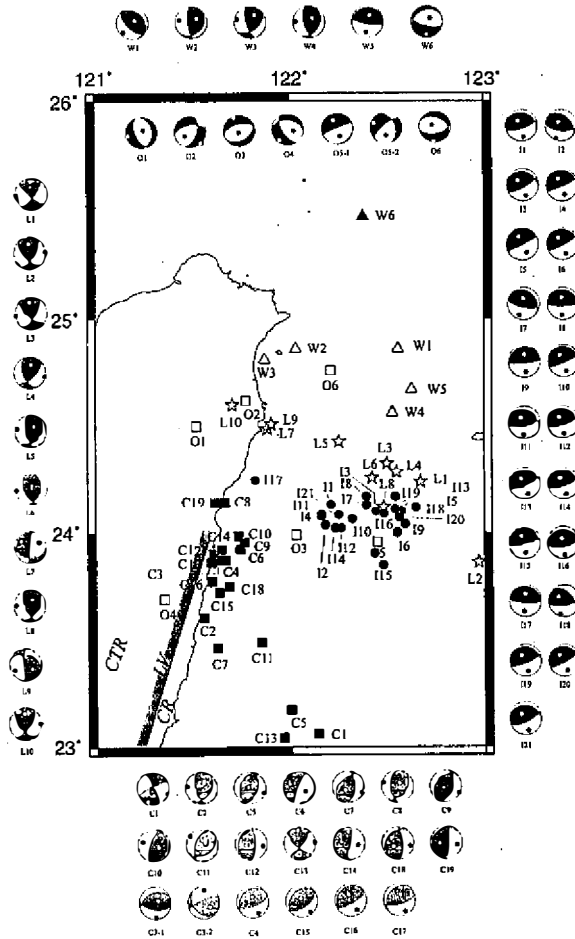
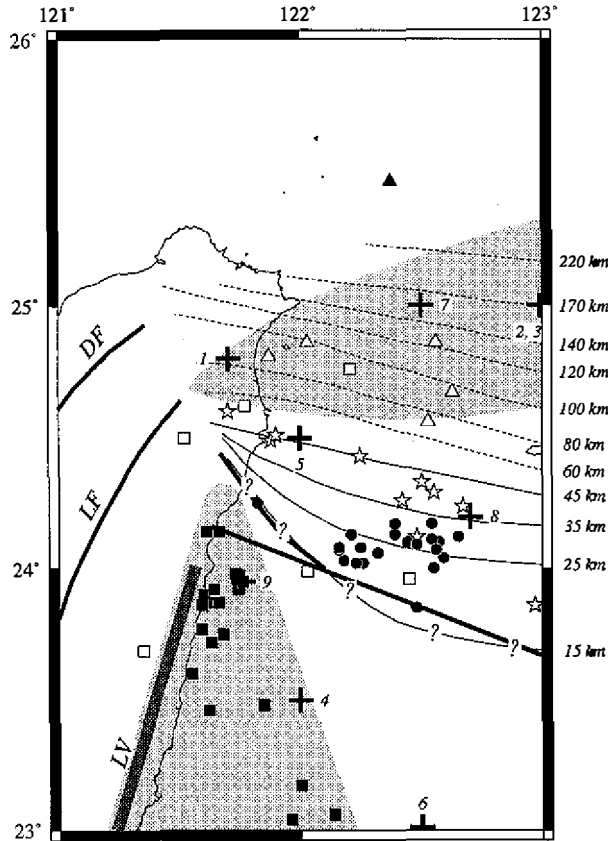


Fig. 2a. Epicenters and focal mechanisms of earthquakes occurred in the study region. Results are adapted from Kao *et al.* (1998). Equal-area projections of the lower-hemispheres of the focal spheres for 62 earthquakes are plotted showing the orientation of the nodal planes, as well as that of the *P* (solid circles) and *T* axes (open circles). Darkened areas show quadrants with compressional *P* wave first motions. Five major seismogenic structures are delineated, as indicated by different symbols and shadings for epicenters and inside the darken quadrants, respectively: Collision Seismic Zone (CSZ, solid squares), Interface Seismic Zone (ISZ, solid circles), Wadati-Benioff Seismic Zone (WBSZ) showing downdip extension (open triangles) and compression (solid triangle), Lateral Compression Seismic Zone (LCSZ, open stars), Okinawa Seismic Zone (OSZ) and normal-faulting earthquakes (open squares). The Central Range (CTR) and Coastal Range (CR) are, respectively, located to the west and east of the Longitudinal Valley (LV; shaded line).



*Fig. 2b.* Inferred configuration of seismogenic structures in the study region. Symbols for earthquakes are the same as in Figure 2a. Big crosses indicate historic large and great earthquakes listed in Table 2. The CSZ (the large shaded triangular zone) is a predominant seismogenic structure in the region. The ISZ is significantly distorted at its westernmost end, as indicated by the thin solid isodepth contours between 15 and 45 km (Kao *et al.*, 1998). Our data have limited constraint on part of the 15 km depth contour, as marked by the question marks. The WBSZ is striking  $\sim 110^\circ$  as shown by dashed isodepth contours of the top of the subducted slab. The LCSZ is located between ISZ and WBSZ from northeast Taiwan to the eastern edge of our study region. The OSZ (shaded area between  $\sim 24.5^\circ\text{N}$  and  $\sim 25^\circ\text{N}$ ) extends westward into northeast Taiwan. Locations of the deformation front (DF) in west Taiwan and the Lishan fault (LF) are adapted from Ho (1988). Location of a possible tear fault in the region is marked by a thick solid line labeled with 'TF' (Lallemand *et al.*, 1997). Based on our results, its western segment might locate slightly to the north, as indicated by the line with question marks.

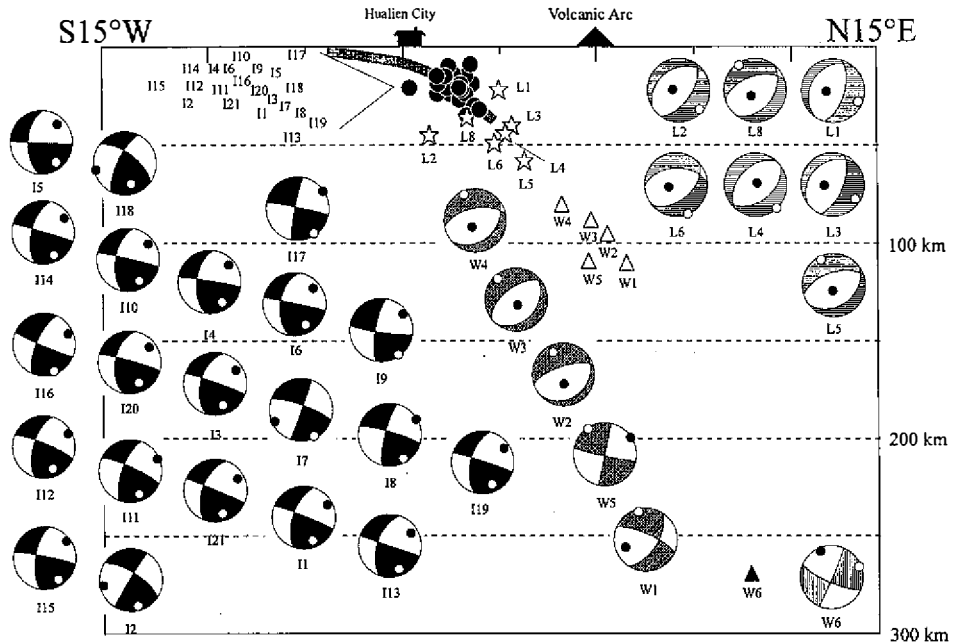


Fig. 2c. N15°E-S15°W cross section (without vertical exaggeration). Hypocenters (small symbols) and focal mechanisms (large spheres) of earthquakes provide an outline of the configuration of the subducted Philippine Sea plate. Fault plane solutions are shown in equal-area projections of the back hemispheres of the focal sphere. Symbols are the same as in Figure 2a. Dashed lines mark depths at 50 km intervals. Earthquakes associated with low-angle thrust faulting, presumably representing the location of plate interface (thick shaded curve), occurred over limited depths between 10 and 35 km. A group of earthquakes showing lateral compression (L1-L10) is found between the interface events and the Wadati-Benioff zone, probably due to the collision-related lateral compression.

Generally speaking, earthquakes with depths less than ~70 km occurred in 4 distinct seismogenic structures. The most prominent one is the CSZ, characterized by numerous earthquakes that occurred along the eastern coast and offshore with thrust or strike-slip faulting. The orientations of *P*-axes for these events are consistently in either E-W or NW-SE directions, presumably resulting from the collision between PSP and EP. The focal depths show a clear bimodal distribution with peaks at 0-20 km and 30-40 km, respectively. The northern terminus of CSZ is located somewhere between Ilan and Hualien where it connects to the western boundary of the interplate seismic zone (Figures 1 and 2).

The geometry of plate interface in this region is rather complex. To the east of ~122°E, it is represented by a group of earthquakes showing typical low-angle thrust mechanisms (ISZ,

Table 1. Summary of earthquake source parameters used in this study.

Event <sup>a</sup>	Date	O. T. <sup>b</sup> , UT	Lat. <sup>b</sup> , °N	Lon. <sup>b</sup> , °E	Depth <sup>c</sup> , km	P Axis Az. <sup>d</sup> , Pl. <sup>d</sup> , deg	T Axis Az. <sup>d</sup> , Pl. <sup>d</sup> , deg	Strike, deg	Dip, deg	Rake, deg	$m_b^b$	Seismic Moment, $\times 10^{17}$ N m
<i>Collision Seismic Zone (CSZ)</i>												
C1	Jan. 25, 1972	03:41:24.0	23.06	122.14	14	110, 4	201, 10	336	86	10	6.0	1340
C2	April 24, 1972	09:57:21.2	23.60	121.55	17(4.0) $\pm$ 4	277, 11	27, 61	36 $\pm$ 11	41 $\pm$ 4	132 $\pm$ 6	6.1	164 $\pm$ 23
C3	Nov. 9, 1972	18:41:13.0	23.87	121.61	16(0.5) $\pm$ 4	177, 10	56, 71	100 $\pm$ 6	57 $\pm$ 3	109 $\pm$ 5	5.9	12.5 $\pm$ 4.2
					2(0.5) $\pm$ 9	2, 25	125, 49	137 $\pm$ 6	33 $\pm$ 21	155 $\pm$ 12		13.6 $\pm$ 9.0
C4	Nov. 21, 1972	02:47:16.4	23.87	121.66	8(1.0) $\pm$ 6	153, 22	357, 66	70 $\pm$ 4	68 $\pm$ 3	100 $\pm$ 7	5.5	5.46 $\pm$ 1.870
					21(1.0) $\pm$ 10	144, 28	20, 47	78 $\pm$ 12	80 $\pm$ 7	121 $\pm$ 28		1.60 $\pm$ 0.80
C5	Dec. 23, 1978	11:23:13.7	23.17	122.00	18	110, 5	290, 85	200	40	90	6.5	190
C6	Jan. 23, 1982	14:10:40.7	23.92	121.74	12(3.0) $\pm$ 7	119, 52	292, 38	205 $\pm$ 4	83 $\pm$ 4	-87 $\pm$ 10	5.6	7.22 $\pm$ 1.3
C7	March 22, 1986	04:45:32.8	23.46	121.62	33	113, 6	216, 67	226	44	123	5.6	8.5
C8	May 20, 1986	05:25:48.4	24.14	121.66	22(1.0) $\pm$ 4	286, 8	38, 68	179 $\pm$ 11	56 $\pm$ 6	66 $\pm$ 7	6.1	33.6 $\pm$ 4.4
					22(1.0) $\pm$ 5	122, 21	4, 49	169 $\pm$ 18	37 $\pm$ 9	27 $\pm$ 13		9.83 $\pm$ 3.73
C9	Nov. 14, 1986	21:20:05.6	23.95	121.76	33(1.0) $\pm$ 8	117, 7	237, 78	17 $\pm$ 6	52 $\pm$ 3	77 $\pm$ 4	6.1	1150 $\pm$ 273
C10	Jan. 6, 1987	05:07:48.1	23.98	121.73	38(1.0) $\pm$ 5	287, 29	114, 60	199 $\pm$ 12	74 $\pm$ 5	93 $\pm$ 15	5.8	3.84 $\pm$ 0.70
					31(1.0) $\pm$ 9	231, 1	142, 48	175 $\pm$ 16	58 $\pm$ 11	141 $\pm$ 18		2.59 $\pm$ 0.70
C11	April 24, 1988	20:03:29.2	23.48	121.85	41	307, 8	62, 71	202	55	69	5.5	1.7
C12	July 20, 1988	23:15:36.7	23.90	121.60	36(1.0) $\pm$ 4	100, 25	258, 64	3 $\pm$ 9	70 $\pm$ 4	81 $\pm$ 11	5.8	7.73 $\pm$ 2.80
C13	Aug. 3, 1989	11:31:20.4	23.04	121.96	9(3.5) $\pm$ 5	85, 5	353, 22	131 $\pm$ 5	71 $\pm$ 6	12 $\pm$ 5	5.9	33.2 $\pm$ 9.2
C14	Dec. 13, 1990	03:01:48.0	23.92	121.64	6(1.0) $\pm$ 4	100, 42	284, 48	12 $\pm$ 11	87 $\pm$ 4	92 $\pm$ 16	5.9	57.0 $\pm$ 16.0
C15	Dec. 13, 1990	19:50:17.9	23.72	121.63	10(1.0) $\pm$ 4	142, 11	345, 79	56 $\pm$ 5	57 $\pm$ 4	95 $\pm$ 7	5.9	20.6 $\pm$ 9.0
C16	Dec. 25, 1990	14:21:53.2	23.77	121.59	8(0.5) $\pm$ 5	146, 27	340, 62	61 $\pm$ 5	73 $\pm$ 4	96 $\pm$ 12	5.6	5.93 $\pm$ 2.10
					14(0.5) $\pm$ 10	128, 42	324, 46	45 $\pm$ 10	88 $\pm$ 6	98 $\pm$ 23		1.94 $\pm$ 0.84
C17	April 19, 1992	18:32:00.2	23.86	121.59	14(0.5) $\pm$ 4	153, 20	13, 64	76 $\pm$ 13	67 $\pm$ 7	107 $\pm$ 13	5.8	13.0 $\pm$ 4.5
C18	Sept. 1, 1992	16:41:13.4	23.75	121.68	63(2.0) $\pm$ 4	102, 19	234, 62	221 $\pm$ 10	31 $\pm$ 6	130 $\pm$ 8	6.0	5.88 $\pm$ 1.50
C19	Feb. 23, 1995	05:19:01.9	24.14	121.61	34 $\pm$ 4	103, 32	262, 56	5 $\pm$ 6	78 $\pm$ 4	80 $\pm$ 11	5.9	11.8 $\pm$ 1.4
<i>Interface Seismic Zone (ISZ)</i>												
I1	Jan. 13, 1968	07:03:45.8	24.13	122.21	27(3.3) $\pm$ 4	172, 26	321, 60	71 $\pm$ 4	73 $\pm$ 3	76 $\pm$ 7	5.7	17.2 $\pm$ 1.8
I2	Feb. 16, 1971	14:26:10.8	24.03	122.18	24 $\pm$ 5	202, 11	321, 68	96 $\pm$ 5	59 $\pm$ 4	68 $\pm$ 6	5.7	5.53 $\pm$ 0.48
I3	April 17, 1972	10:49:44.4	24.10	122.44	22(4.0) $\pm$ 4	164, 30	312, 55	62 $\pm$ 5	77 $\pm$ 3	74 $\pm$ 7	5.8	14.4 $\pm$ 2.0
					15(4.0) $\pm$ 6	187, 25	307, 48	72 $\pm$ 5	77 $\pm$ 4	57 $\pm$ 7		8.93 $\pm$ 2.0
I4	July 15, 1977	02:12:56.6	24.07	122.16	15	164, 38	328, 50	67	84	82	5.6	6.8
I5	Feb. 8, 1978	00:15:40.5	24.10	122.57	15	154, 42	334, 48	64	87	90	5.5	14
I6	March 14, 1978	20:32:16.9	24.00	122.55	15	161, 36	323, 52	63	82	81	5.5	6.7
I7	June 21, 1983	14:48:07.9	24.13	122.39	24(4.0) $\pm$ 5	202, 24	353, 63	102 $\pm$ 6	70 $\pm$ 6	78 $\pm$ 10	5.8	26.4 $\pm$ 5.0
					24(4.0) $\pm$ 9	215, 3	123, 43	161 $\pm$ 9	63 $\pm$ 10	145 $\pm$ 14		17.3 $\pm$ 8.5
I8	June 24, 1983	09:06:46.3	24.17	122.39	30(4.0) $\pm$ 4	187, 30	343, 58	88 $\pm$ 8	76 $\pm$ 5	79 $\pm$ 12	6.0	104 $\pm$ 14
					31(4.0) $\pm$ 7	178, 37	6, 53	91 $\pm$ 13	82 $\pm$ 7	94 $\pm$ 19		20.0 $\pm$ 8.0
I9	June 25, 1983	19:40:54.0	24.04	122.59	14	172, 35	0, 55	85	80	94	5.5	1.74
I10	Sept. 7, 1983	23:11:59.4	24.06	122.32	10	166, 35	325, 53	67	81	80	5.5	2.65
I11	Sept. 21, 1983	19:20:44.4	24.08	122.16	21(3.0) $\pm$ 5	183, 24	321, 60	78 $\pm$ 6	71 $\pm$ 3	71 $\pm$ 12	6.0	28.9 $\pm$ 3.3
I12	Sept. 23, 1983	12:29:23.4	24.02	122.26	19(3.0) $\pm$ 6	177, 27	318, 56	72 $\pm$ 5	75 $\pm$ 4	71 $\pm$ 11	5.8	3.93 $\pm$ 0.44
					44(3.0) $\pm$ 12	95, 21	350, 34	40 $\pm$ 11	82 $\pm$ 7	139 $\pm$ 17		3.10 $\pm$ 0.60
I13	March 28, 1984	09:11:21.0	24.11	122.54	35(4.0) $\pm$ 9	164, 28	321, 60	66 $\pm$ 6	74 $\pm$ 5	80 $\pm$ 11	5.5	7.97 $\pm$ 1.01
I14	Feb. 27, 1986	06:23:13.3	24.02	122.23	15	167, 31	326, 57	69	77	80	5.8	5.7
I15	Feb. 12, 1988	19:15:35.4	23.85	122.48	21(4.0) $\pm$ 11	175, 37	336, 51	76 $\pm$ 8	82 $\pm$ 8	81 $\pm$ 17	5.6	1.40 $\pm$ 0.32
I16	Aug. 21, 1989	23:12:41.4	24.09	122.48	19(3.0) $\pm$ 5	171, 22	342, 68	78 $\pm$ 4	67 $\pm$ 3	86 $\pm$ 5	5.6	25.7 $\pm$ 7.0
I17	July 16, 1990	19:14:51.7	24.25	121.82	9(1.0) $\pm$ 6	187, 34	358, 56	296 $\pm$ 20	12 $\pm$ 6	112 $\pm$ 20	5.5	2.84 $\pm$ 1.20
I18	Sept. 28, 1992	14:06:02.6	24.12	122.65	19(3.0) $\pm$ 5	198, 13	305, 54	323 $\pm$ 10	44 $\pm$ 5	143 $\pm$ 6	5.8	12.0 $\pm$ 2.70
					19(3.0) $\pm$ 5	138, 22	342, 66	211 $\pm$ 19	24 $\pm$ 6	67 $\pm$ 16		11.0 $\pm$ 2.6
I19	May 23, 1994	05:36:01.6	24.17	122.54	32(3.0) $\pm$ 3	168, 31	323, 56	68 $\pm$ 14	77 $\pm$ 7	78 $\pm$ 14	5.7	12.7 $\pm$ 4.4
I20	May 23, 1994	15:16:57.1	24.07	122.56	21(3.0) $\pm$ 4	163, 35	317, 52	62 $\pm$ 4	81 $\pm$ 3	77 $\pm$ 8	6.0	5.16 $\pm$ 1.0
					35(3.0) $\pm$ 2	171, 27	318, 59	69 $\pm$ 7	74 $\pm$ 5	75 $\pm$ 11		4.12 $\pm$ 1.60
I21	April 3, 1995	11:54:43.6	24.08	122.25	24	166, 26	315, 61	65	72	76	5.7	3.7
<i>Wadati-Benioff Seismic Zone (WBSZ)</i>												
W1	July 1, 1966	05:50:38.0	24.86	122.56	110(0.5) $\pm$ 4	225, 17	44, 73	135 $\pm$ 8	62 $\pm$ 4	90 $\pm$ 8	6.1	46.4 $\pm$ 5.37
W2	Oct. 9, 1971	13:15:38.5	24.86	122.03	95 $\pm$ 8	282, 25	57, 56	175 $\pm$ 8	73 $\pm$ 6	68 $\pm$ 10	5.7	3.72 $\pm$ 0.42
W3	Sept. 2, 1978	01:57:34.2	24.81	121.87	88	284, 14	29, 46	54	47	152	6.0	80
W4	Dec. 17, 1982	02:43:03.8	24.56	122.53	80(2.0) $\pm$ 7	272, 17	40, 64	29 $\pm$ 10	33 $\pm$ 6	128 $\pm$ 8	5.9	4.40 $\pm$ 0.9
W5	April 26, 1983	15:26:40.2	24.67	122.63	115(2.0) $\pm$ 5	186, 33	17, 52	101 $\pm$ 4	78 $\pm$ 4	95 $\pm$ 7	5.7	6.03 $\pm$ 0.34
W6	Feb. 13, 1984	04:48:57.7	25.47	122.38	269(4.0) $\pm$ 9	39, 64	183, 22	104 $\pm$ 16	69 $\pm$ 9	-75 $\pm$ 17	5.5	2.35 $\pm$ 1.50
<i>Lateral Compressional Seismic Zone (LSZ)</i>												
L1	March 12, 1966	16:31:19.9	24.24	122.67	22	263, 2	354, 23	36	73	165	6.6	4860
L2	March 23, 1966	00:04:33.4	23.86	122.97	45(4.0) $\pm$ 4	85, 1	354, 42	31 $\pm$ 5	63 $\pm$ 3	147 $\pm$ 4	6.3	27.5 $\pm$ 1.9
L3	May 5, 1966	14:21:22.3	24.33	122.50	40	259, 1	350, 31	129	70	24	5.6	-
L4	May 28, 1966	00:03:59.2	24.29	122.55	44(0.5) $\pm$ 5	104, 5	9, 48	46 $\pm$ 5	62 $\pm$ 6	139 $\pm$ 7	5.5	6.30 $\pm$ 0.49
L5	Oct. 25, 1967	00:59:23.3	24.43	122.25	58(2.0) $\pm$ 5	278, 14	36, 62	37 $\pm$ 3	37 $\pm$ 3	152 $\pm$ 5	6.0	205 $\pm$ 44
L6	Nov. 27, 1970	09:39:24.1	24.26	122.24	49(1.5) $\pm$ 6	261, 6	7, 69	11 $\pm$ 13	42 $\pm$ 10	115 $\pm$ 14	5.7	3.94 $\pm$ 0.80
L7	Jan. 29, 1981	04:51:37.4	24.49	121.88	15	61, 35	304, 33	183	88	-128	5.7	10
L8	Jan. 13, 1985	21:51:22.5	24.12	122.48	36	269, 15	22, 56	156	66	57	5.8	1.73
L9	June 5, 1994	01:09:30.1	24.51	121.90	8(1.0) $\pm$ 4	242, 23	125, 47	178 $\pm$ 5	76 $\pm$ 4	125 $\pm$ 9	6.1	32.8 $\pm$ 14.0
L10	June 25, 1995	06:59:06.2	24.60	121.70	47(1.0) $\pm$ 6	90, 6	355, 39	36 $\pm$ 4	68 $\pm$ 3	146 $\pm$ 5	5.8	6.98 $\pm$ 1.90

Okinawa Seismic Zone (OSZ) and Normal-Faulting Earthquakes

Table 1. Continued

O1	May 10, 1983	00:15:05.0	24.50	121.52	7(3.0) $\pm$ 4	36, 77	256, 10	159 $\pm$ 11	55 $\pm$ 8	-100 $\pm$ 10	5.6	3.48 $\pm$ 0.62
					30(3.0) $\pm$ 7	38, 11	131, 15	174 $\pm$ 17	72 $\pm$ 9	177 $\pm$ 14		2.19 $\pm$ 0.80
O2	July 30, 1986	11:31:48.9	24.62	121.77	14 $\pm$ 5	230, 53	140, 0	19 $\pm$ 16	56 $\pm$ 9	-136 $\pm$ 15	5.6	1.60 $\pm$ 0.60
					20 $\pm$ 5	219, 76	28, 14	114 $\pm$ 18	31 $\pm$ 11	-95 $\pm$ 16		1.39 $\pm$ 0.60
O3	April 11, 1987	18:13:28.3	23.99	122.03	14(2.0) $\pm$ 6	198, 79	340, 9	62 $\pm$ 10	37 $\pm$ 4	-102 $\pm$ 7	5.6	5.96 $\pm$ 0.90
O4	Jan. 18, 1991	01:36:26.7	23.69	121.35	5 $\pm$ 3	105, 60	218, 13	149 $\pm$ 8	63 $\pm$ 7	-60 $\pm$ 11	5.9	3.70 $\pm$ 0.98
O5	May 24, 1994	04:00:42.1	23.96	122.45	35(3.0) $\pm$ 7	162, 49	334, 41	248 $\pm$ 5	86 $\pm$ 3	-86 $\pm$ 10	6.2	36.5 $\pm$ 9.6
					10(3.0) $\pm$ 4	180, 49	293, 18	229 $\pm$ 7	72 $\pm$ 4	-53 $\pm$ 7		34.9 $\pm$ 6.2
O6	Oct. 28, 1994	23:51:12.2	24.76	122.21	33	297, 72	186, 7	81	54	-111	5.5	3.3

<sup>a</sup>Events are numbered in chronological order. Results for each subevent are given in successive rows.

<sup>b</sup>Epicenters (Lat., latitude; Lon., longitude), origin times (O. T.), and magnitudes are those reported in the *Bulletin of the International Seismological Centre* (ISC) and the *Preliminary Determination of Epicenters* (PDE) for events before and after 1988, respectively.

<sup>c</sup>Depth below sea level. Where applicable, the value inside parentheses is the thickness of the water column above the source region.

<sup>d</sup>Az., azimuth; Pl., plunge.

Table 1 and Figure 2a). To the west of 122°E, however, only one low-angle thrust event is observed (event I17). Moreover, this event has a very shallow focal depth (9 $\pm$ 6 km), making it stand out from the plate interface inferred from the remaining low-angle thrust events (Figure 2). Combining with the distribution of local seismicity, Kao *et al.* (1998) interpreted that the plate interface has been pushed by the northward component of the regional collision (Figure 2b), thus causing the western boundary of the plate interface to distort significantly as it approaches Taiwan.

From the cross section in Figure 2c, it is interesting to point out that the depth distribution of ISZ earthquakes has characteristics quite different from that observed along the rest of Ryukyu arc (Kao and Chen, 1991) and from subduction zones in the western Pacific such as the Japan and Kuril arcs (Kao and Chen, 1995, 1996). While most of the interface events take place between 30 and 50 km along the Ryukyu arc, the seismogenic portion of plate interface in this region is significantly shallower at ~10–35 km. Such a depth range is also shorter than the ~15–45 km and ~15–50 km depth ranges observed for the Japan arc and Kuril–Kamchatka arc, respectively.

In the vicinity of the plate interface, there are some earthquakes showing *P*-axes roughly parallel to the local strike of the arc (LCSZ, events L1–L10; Figure 2). These events are interpreted as a consequence of collision, similar to those of CSZ except that they represent the compressive strain transmitted laterally through the lithosphere. The western end of this structure coincides with that of the interplate thrust zone and the northern tip of CSZ between Ilan and Hualien (Figures 1 and 2).

Normal faulting earthquakes in the region can be related to several different tectonic processes. The OSZ is characterized by a group of shallow events distributed in the Okinawa trough and beneath NE Taiwan (events O1, O2, and O6). The orientation of *T*-axes shows a systematic rotation from ~N–S in the Okinawa trough, which is consistent with the inferred direction of extension (Sibuet *et al.*, 1987), to NW–SE and almost E–W near the northwestern coast and inland, respectively. We shall discuss the tectonic implications of such a pattern in a later section.

Two events (events O3 and O5) are observed to the south of the cluster of ISZ earthquakes with *T*-axes trending ~N–S (Figure 2a). Their epicenters are located to the north of the Ryukyu trench rather than in the so-called outer-rise region. Similar earthquakes are also

observed along the rest of Ryukyu arc and can be explained by the plate bending effect transmitted from the outer-rise to the vicinity of trench (Kao and Chen, 1991). One normal event (O4) took place to the west of the Longitudinal Valley with a  $T$ -axis approximately parallel to the local structural trend, perpendicular to the maximum compressive stress direction (Figure 2a). By the analogy to the high Tibet plateau, this event presumably reflects the lateral extension located behind the main collision zone (e.g., England and Houseman, 1989).

### 3. SEISMOGENIC CONDITIONS ALONG THE PLATE INTERFACE

The majority of the world's great earthquakes are associated with the interplate thrust zone (Kelleher *et al.*, 1974; Jarrard, 1986). Since global seismological observation began in early 1960's, there has been extensive research efforts to delineate the relationship between seismogenic conditions along the plate interface and physical/tectonic parameters in various subduction zones (e.g., Astiz and Kanamori, 1986; Christensen and Ruff, 1983, 1988; Furukawa, 1993; Kanamori, 1977; Kelleher *et al.*, 1973, 1974; McCaffrey, 1993, 1994; Pacheco and Sykes, 1992; Pacheco *et al.*, 1993; Ruff, 1989; Ruff and Kanamori, 1983; Scholz and Campos, 1995; Suárez and Sánchez, 1996; Tichelaar and Ruff, 1991). In this section, we shall address the seismogenic conditions for the interface between PSP and EP in the southernmost Ryukyu arc-Taiwan region from four different points of view: (1) historic major earthquakes in the region, (2) seismic coupling along the plate interface, (3) geometric configuration of the plate interface, and (4) interplate slip partitioning.

#### 3.1 Historic Major Earthquakes in the Region

There have been several compilations in the literature for historic large and great earthquakes that have occurred in subduction zones. Duda (1992) systematically recalibrated magnitudes for all large and great earthquakes ( $M_s \geq 7.0$ ) between 1903 and 1985 using historic seismograms preserved at the Seismological Observatory of Göttingen University, Germany. The result was compiled together with 16 other catalogs published in the literature and is probably the most complete catalog as far as major earthquakes of this century are concerned. Combining this catalog and the more recent bulletins of International Seismological Center (ISC) and Preliminary Determination of Epicenters (PDE), we search for large and great earthquakes which occurred in the study region and present the result in Table 2 and Figure 2b.

As pointed out by Duda (1992), magnitudes of historic earthquakes (i.e., before the early 1960's when the World-Wide Standardized Seismographic Network was established) determined by different researchers using various phases and techniques often result in inconsistent values. Therefore, estimating the possible uncertainty becomes the first step toward a meaningful interpretation. Taking the largest event in the region (June 5, 1920) for example, Gutenberg and Richter (1954) reported the  $M_s$  to be 8.0 based on 20 s period surface waves. Other estimates range from 7.8 (Abe, 1981; Geller and Kanamori, 1977) to 8.3 (Richter, 1958; Duda, 1965). Duda's (1992) catalog lists the body- and surface-wave magnitudes to be 6.9–7.9 and 8.0–8.2, respectively, and relates most of the differences to the choice of different calibration functions. Since the amplitudes of body or surface waves become saturated once the rupture area of a fault is comparable to the corresponding wavelength, as for the cases of

Table 2. Large and great earthquakes in the study region since 1903.

No.	Date	Lat. <sup>1</sup>	Long. <sup>1</sup>	$M_b^1$	$M_s^1$	$M_w$ , ref <sup>3</sup>
1	June 7, 1903	24.8	121.7	-	-	7.8, UAI
2	April 12, 1910	25.0	123.0	6.5	-	7.8, G&R
3	July 4, 1917	25.0	123.0	6.5	7.8	7.5, UAI
4	June 5, 1920	23.5	122.0	6.9	8.2	8.0, G&R
5	Sept. 1, 1922	24.5	122.0	-	7.9	7.6, G&R
6	Nov. 24, 1951	23.0	122.5	6.9	7.7	7.3, G&R
7	April 26, 1959	25.0	122.5	6.5	-	7.7, UAI
8	March 12, 1966	24.24 <sup>2</sup>	122.67 <sup>2</sup>	6.6 <sup>2</sup>	8.0	7.8, ABE
9	Nov. 14, 1986	23.95 <sup>2</sup>	121.76 <sup>2</sup>	6.1 <sup>2</sup>	7.7 <sup>2</sup>	-

<sup>1</sup> Values reported by Duda (1992) unless otherwise noted.

<sup>2</sup> Values reported in the bulletins of the *International Seismological Center (ISC)*.

<sup>3</sup> UAI: *Usami* (1981); G&R: *Gutenberg and Richter* (1954); ABE: *Abe* (1981).

large and great earthquakes, Kanamori (1978) proposed a more appropriate magnitude scale based on an earthquake's scalar seismic moment (*i.e.*, moment magnitude,  $M_w$ ). For example, a large thrust event which occurred on November 14, 1986 (event C9; Figure 2a, Tables 1 and 2) has a reported body- and surface-wave magnitudes of 6.1 and 7.7, respectively. The estimated seismic moment of  $1.15 \times 10^{20}$  N m (Table 1) corresponds to a  $M_w$  of 7.3, which seems to better characterize the overall physical size of the event. Kanamori (1978) compared the estimated  $M_s$  and  $M_w$  for ten of the largest earthquakes of this century and found that the most differences are less than 0.6. Exceptions are the 1952 Kuril, the 1960 Chile, and the 1964 Alaska earthquakes; all took place along regions considered to be strongly coupled. Although there is no report on seismic moment for historic earthquakes occurred in the study area, it is probably justifiable to assume that the  $M_w$  of a shallow large/great earthquake is within  $\pm 0.5$  of the estimated  $M_s$ , providing that the Ryukyu arc is not strongly coupled (a subject we shall address in the next section).

On the other hand, it is very difficult to access possible epicentral mislocations associated with historic events. As demonstrated in previous section, seismogenic structures in this region are rather complicated such that at least 4 major seismic zones exist at shallow depth. From the listed earthquake locations alone without precise knowledge of the focal depths and mechanisms, it is nearly impossible to tell along which seismogenic structures the historic earthquakes took place.

Generally speaking, there seems no doubt that at least a few earthquakes with  $M_w \geq 7.0$ –7.5 have occurred in the southernmost Ryukyu arc–Taiwan region since the turn of this century. Whether or not these events occurred along the interplate thrust zone, as expected for most major subduction zone earthquakes (Kanamori, 1970), however, is quite uncertain. Based on the present-day seismic patterns (Figure 2), it is equally possible that these events belong to

ISZ, CSZ, or OSZ.

### 3.2 Seismic Coupling Along the Plate Interface

Since the 1970's when the concept of "seismic coupling" was first introduced by Kanamori (1977), it has been extensively used to explain the occurrence of large/great earthquakes in subduction zones. The basic idea is that the relative slip between two plates across a plate interface is controlled by a temporal stick-and-slip behavior (*i.e.*, coupled-and-uncoupled cycle). The plate interface slips during large/great subduction zone earthquakes (uncoupled process), but sticks during interseismic period (coupled process). Such an alternative pattern is reflected by the changing focal mechanisms in the vicinity of plate interface, including earthquakes in the outer-rise region (Christensen and Ruff, 1983, 1988) and within the Wadati-Benioff zone at intermediate depth (Astiz and Kanamori, 1986; Astiz *et al.*, 1988; Dmowska *et al.*, 1988; Lay *et al.*, 1989). As depicted in Figure 3a, compressive and downdip extensional earthquakes are observed in the outer-rise and at intermediate depth, respectively, when the interface is strongly coupled. The strain regimes will switch to outer-rise extension and downdip compression at intermediate depth immediately after the occurrence of a great subduction zone earthquake. As the interface is locked again and accumulating seismogenic strain, the switched strain regimes would gradually return to their original state and the cycle renews.

On the other hand, many subduction zones have no signature of temporal patterns in either the outer-rise region or at intermediate depth (e.g., Astiz *et al.*, 1988; Christensen and Ruff, 1988; Kao and Chen, 1995, 1996). The most accepted interpretation is that the corresponding plate interface is uncoupled such that the observed strain pattern reflects the spatial distribution of various tectonic processes (Figure 3b). For example, extensional earthquakes observed in the outer-rise with *T*-axes in the plate convergence direction represent the plate bending, while downdip extension and/or compression at intermediate depth probably manifest the interaction between the subducted lithosphere and the surrounding asthenosphere (Isacks and Molnar, 1969, 1971). In this scenario, no great earthquakes are expected to take place along the plate interface.

In this study, we have found no compressional but two extensional earthquakes (events O3 and O5) in the vicinity of trench and plate interface. The significance of such a pattern is two-folded. First, the epicentral locations of the extensional events are not to the ocean side of the trench where the bending stress is expected to be maximum, but shift more than 50 km toward the arc (Figure 2). This is similar to that found in the rest of Ryukyu arc and can be explained by a relatively weak coupling along the seismogenic portion of the interface such that the bending (extensional) stress is allowed to transmit beyond the trench (Kao and Chen, 1991). Secondly, the lack of outer-rise compressional events implies that the current state of strain along the plate interface is not immediately before the occurrence of a great subduction zone earthquake (Figure 3a). In fact, it is inconclusive from the existence of extensional earthquakes alone to determine whether a seismic cycle indeed exists due to the short time window of modern seismological observation. The mechanical state of the interface can either be weakly coupled with no variation with respect to time (*i.e.*, a purely spatial pattern, Figure 3b), or weakly to immediately coupled during the interseismic period of a seismic cycle

(Figure 3a).

In a strongly coupled subduction zone such as the Kuril–Kamchatka arc, there were not only occurrences of outer-rise compressional events and historic great subduction zone earthquakes but also a systematic variation of focal mechanisms for events occurred along the

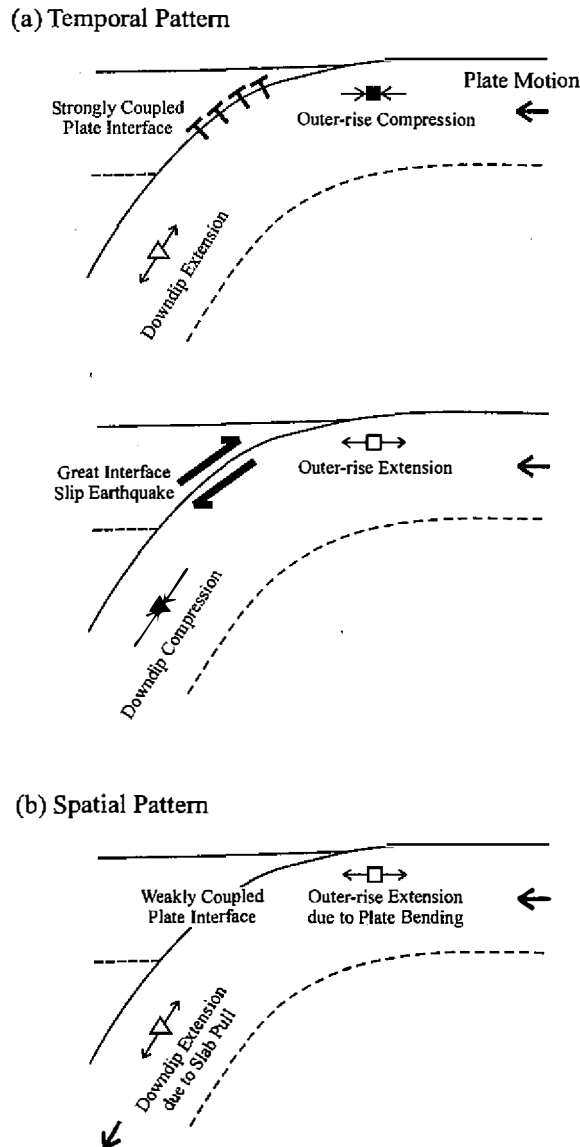


Fig. 3. Schematic diagrams showing strain patterns associated with (a) a temporal cycle due to coupling/uncoupling along the plate interface and (b) spatial distribution of various tectonic processes.

lower portion of the seismogenic interface. Kao and Chen (1995) reported that while these events are still thrust-faulting, the dip angles derived from focal mechanisms are consistently larger than that of the plate interface. From detailed waveform modeling, it is concluded that these so-called "transitional thrust" events must have occurred within the subducted oceanic crust below the plate interface, probably due to the strong coupling (*i.e.*, locked) along the interface at depths between 30 and 50 km. Since we found no systematic dip increase for ISZ earthquakes in the study region with respect to depth, it seems to suggest that the plate interface is not seismically locked.

### 3.3 Geometric Configuration of the Plate Interface

According to elastic dislocation theory (Aki and Richards, 1980), seismic moment is defined as  $M_o = \mu DS$  where  $\mu$  is the rigidity of the material surrounding the fault,  $D$  is the average displacement on the fault plane, and  $S$  is the rupture area of the fault. Consequently, a great earthquake requires a sizable fault and/or big dislocation across the fault plane. Taking an earthquake of  $M_w \sim 8$  for example, the corresponding moment release is estimated at  $1.3 \times 10^{21}$  N m. If we assume a typical  $\mu$  of  $3.5 \times 10^{10}$  N m<sup>-2</sup> and  $D$  of 3.5 m (the average amount of slip for large and great interface earthquakes (Delouis *et al.*, 1997)), then the inferred rupture area is  $\sim 10^4$  km<sup>2</sup> which is equivalent to a fault of approximately 40 km by 250 km in dimension.

Such a large rupture area is inconsistent with the geometrical configuration of the inferred plate interface. Specifically, the geometry of the interplate thrust zone turns from striking NE–SW in southern Ryukyu to nearly E–W near Taiwan and results in a prominent setting of oblique subduction. Moreover, it bends sharply toward the north due to the northward component of the regional collision (Figure 2b). This pattern is unfavorable for forming a large, coherent faulting area because variations in fault geometry often terminate the rupture propagation (e.g., Velasco *et al.*, 1996). Even if the rupture nucleates at the point of geometric complexity, it seems unlikely to propagate both ways simultaneously because the change of fault geometry would cause inconsistent block motions across the two sides.

From the cross section shown in Figure 2c, it is clear that the present seismogenic portion of the interface is confined between 10 and 35 km. Therefore, the largest possible rupture area for an earthquake occurring along the plate interface in southernmost Ryukyu arc is probably on the order of  $3 \times 10^3$  km<sup>2</sup> (*i.e.*, 25 km by 120 km; Figures 2b and 2c). Based on the same assumed  $\mu$  and  $D$  as before, the largest possible  $M_w$  is inferred to be 7.6–7.7.

The above moment calculation is uncertain by a factor of at least 2, mostly due to the assumed amount of slip associated with large and great earthquakes. A number of studies have argued that slip distribution can be highly heterogeneous across the fault plane with a range from 0 to as large as 10–15 m (Beckers and Lay, 1995; Gao and Wallace, 1995; Ghose *et al.*, 1997; Mellors *et al.*, 1997; Velasco *et al.*, 1996). However, the very large slip usually is confined to a small area rather than throughout the fault (e.g., Velasco *et al.*, 1996). Even as we double the amount of average slip, the maximum size of an interface earthquake is estimated to be  $\sim 7.8$  in  $M_w$ .

### 3. 4 Interplate Slip Partitioning

Under the framework of plate tectonics, the slip directions of earthquakes along the interplate thrust zone tend to agree with that of plate convergence. However, in a subduction zone where the trench normal direction significantly deviates from that of the plate convergence (*i.e.*, oblique subduction), the slip vectors of interface earthquakes may no longer follow the predicted plate motion but turn toward the trench normal (e.g., Allen, 1962; Fitch, 1972) and the transcurrent component of the relative plate convergence is taken up by deformation in the forearc–backarc region (Fitch, 1972), resulting a pattern of slip partitioning.

It is noted that not every oblique subduction zone is associated with prominent slip partitioning (McCaffrey, 1992). For example, in Mariana the slip vectors of interface earthquakes tend to follow the trench normal direction, but in Colombia they are consistent with the relative plate motion (Liu *et al.*, 1995). In the former case, the average slip obliquity (*i.e.*, the angle between average slip vector and trench normal,  $\psi$ ) is essentially 0, whereas in the later case, it is equal to the convergence obliquity (the angle between the plate convergence direction and trench normal,  $\phi$ ). In a series of studies (McCaffrey, 1992, 1993, 1994, 1996), McCaffrey pointed out that for regions with large  $\phi$ , the occurrence of great subduction earthquakes often correlates with little or no slip partition. He proposed a model to explain the observed correlation in terms of the rheological behavior of the fore-arc. If the deformation is more elastic such that both the lateral and trench-normal components of the relative plate motion can be stored as elastic strain, then interplate thrust events result in a slip direction close to the relative plate convergence and a larger magnitude. On the other hand, if the shear strength of the fore-arc is relatively small such that permanent shear deformation in the fore-arc takes place due to the lateral component of the relative plate motion, then the occurrence of interface events could reflect only the trench-normal elastic strain, thus showing slip partitioning.

In our study region, the convergence obliquity ( $\phi$ ) is as large as  $70\pm 10^\circ$  (Seno *et al.*, 1993; Figure 4). The average slip direction deduced from slip vectors of ISZ earthquakes is  $345\pm 12^\circ$ , which corresponds to a slip obliquity ( $\psi$ ) of  $35^\circ$ . This value is exactly in between the trench normal and relative plate motion directions (Figure 4). Based on McCaffrey's model, the rheological behavior of the Ryukyu fore-arc in this region is not completely elastic, thus is unlikely to generate  $M_w > 8$  subduction earthquakes. Nevertheless, the still significant deviation of slip vector from the trench normal implies that the strength of the fore-arc is not weak, either. Occurrence of major earthquakes with  $M_w > 7.0$  is entirely possible.

Notice that the estimates of slip partitioning, including previous studies of other oblique subduction zones, are all based on global plate motion models. Relative motion of the forearc–backarc system with respect to the rigid interior of subducting/overriding plates is usually included in the analysis (e.g., Yu *et al.*, 1993). For example, the existence of significant backarc spreading would correspond to an average slip vector that is close to the trench normal direction with a speed faster than the relative plate motion. On the other hand, no slip partitioning is expected if the backarc spreading is virtually absent. In our case, the motion of the forearc–backarc system is characterized by a vector pointing NWW relative to the PSP. Such an inference is compatible with the most recent GPS measurements on islets of the southern-

most Ryukyu arc (Imanishi *et al.*, 1996).

#### 4. SEISMOGENESIS DUE TO INTERACTIONS OF DISTINCT STRESS/STRAIN REGIMES

The oblique subduction and collision along eastern Taiwan and offshore obviously has profound effects on the seismogenic patterns in the study region. In this section, we discuss the possible interactions among different stress/strain regimes associated with different tectonic processes.

For example, earthquakes of LCSZ found in the vicinity of plate interface, just above the subducted WBSZ, show consistent orientation of *P*-axes in ~E–W direction (Figure 2b). Eight out of 10 such events also show *T*-axes trending ~N–S either horizontally (which is consistent with the extension within the Okinawa trough) or in slab downdip direction. Therefore, the most straightforward interpretation would be to associate the *P*- and *T*-axes to the compressional strain transmitted laterally within the lithosphere and the extensional strain due to the Okinawa trough opening or the slab pulling force of subducted PSP, respectively.

Another example is shown by the normal events O1 and O2 that occurred in NE Taiwan. Both tomographic and geodetic data indicate that the region is under strong influence of the Okinawa trough opening (Liu, 1995; Rau and Wu, 1995; Yeh *et al.*, 1989). However, the *T*-axis of event O2 is in NW–SE direction, which significantly deviates from the inferred ~N–S extension within the Okinawa trough (Sato *et al.*, 1994; Sibuet *et al.*, 1987). Moving farther inland, event O1 has the *T*-axis in nearly E–W direction. Such a successive rotation of *T*-axes

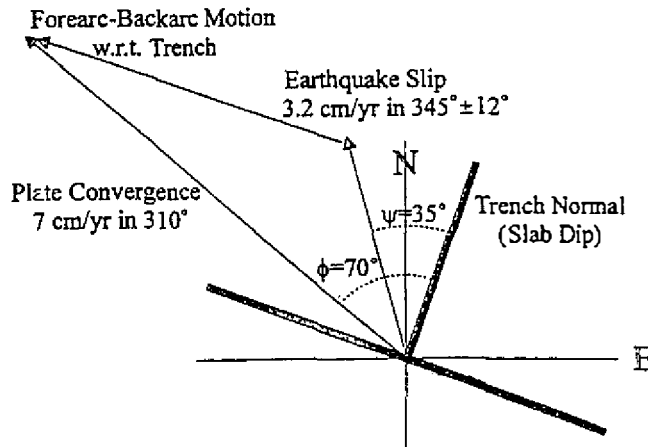


Fig. 4. Slip partition associated with the ISZ earthquakes. The trench normal direction is inferred from the dip of subducted lithosphere. The average earthquake slip direction is in between the inferred trench normal and plate convergence directions. Plate motion and earthquake slip rates are adapted from Kao *et al.* (1998) and Seno *et al.* (1993), respectively.

is interpreted as the consequence of interaction between the extensional regime of the Okinawa trough opening and the compressional regime of the Taiwan Collision Zone along the eastern coast and offshore. Numerical modeling of the regional stress pattern confirms such a standpoint, showing that the direction of maximum tension gradually changes from ~N-S within the Okinawa trough to NW-SE with rapidly decreasing magnitude as it approaches NE Taiwan (Hu and Angelier, 1996).

In Figure 2, notice that all major seismogenic structures extend to NE Taiwan. This makes NE Taiwan the most likely place to have interactions among distinct stress regimes. Although such interactions may not necessarily mean a bigger earthquake, which actually depends on the physical size of the fault, they may increase the frequency of earthquake occurrence because the combined stress regime would reach the failure criteria of geological materials more effectively. Furthermore, because NE Taiwan is very close to the island's capital, the Taipei City, it does not require a great earthquake to cause catastrophic damages. From the seismic hazard point of view, the potential threat from frequent occurrences of  $M_w > 7$  events cannot be ignored.

## 5. DISCUSSION AND IMPLICATIONS

Since the tectonic setting in the southernmost Ryukyu arc-Taiwan region is complex, a legitimate question to ask is whether there exist major seismogenic structures other than those depicted in Figure 2. Lallemand *et al.* (1997) based on detailed bathymetry and seismic profiling data, propose a WNW-trending tear fault within the PSP to explain the ~3 km subsidence of fore-arc basins. The surface projection of the fault roughly follows the inferred plate interface at ~15 km and is marked in Figure 5. The sense of fault slip is along a nearly vertical plane with the northern block moving down. If the fault plane dips steeply toward the south, then the corresponding earthquake focal mechanism is basically identical to a low-angle thrust faulting typical of ISZ events, assuming a double-couple source model. Thus, from earthquake focal mechanisms alone, one cannot exclude the existence of a tear fault for sure.

In their discussion, Kao *et al.* (1998) point out that hypocenters of some ISZ events do not fall exactly along the inferred plate interface. They speculate several possible causes, including distortion or finite thickness of the interplate thrust zone, occurrence of intraplate rather than interplate events, and/or uncertainties in focal depths. From the cross section in Figure 2c, the distribution of earthquake hypocenters is too sparse to neither confirm nor reject the existence of a tear fault at shallow depths. However, if the off-interface event I17 is interpreted as an earthquake occurring along the possible tear fault, then we need to move the inferred western segment of the fault slightly toward the north (solid thick line with question marks in Figure 5), changing the strike from WNW to NW as it approaches Taiwan. Furthermore, since there is no clear bathymetric signature of the tear fault in the region, it is inferred that the fault might be a so-called "blind thrust" buried within the crust and/or uppermost mantle.

Given the conditions that (1) the strike of a possible tear fault might vary along different segments, and (2) the seismogenic portion probably spans no wider than that of the corresponding plate interface, we speculate that the largest earthquake corresponding to this newly inferred structure would probably be similar or smaller than that estimated for the plate inter-

face ( $M_w \sim 7.6-7.7$ ). On the other hand, it is very likely that the stress regime associated with this structure can interact with others in NE Taiwan and result in not necessarily great, but frequent large earthquakes inland or not far offshore.

Results of this study have important implications on the configuration of a seismic early-warning system, should the government decide to upgrade the current one, and the necessary planning/setup for emergency rescue operations once a major damaging earthquake strikes. Since the interaction among different tectonic processes is likely to generate large damaging earthquakes to the island's most populated area than any single seismogenic structure, it is suggested that seismic activity in NE Taiwan, particularly between Ilan and Hualien, should be closely monitored. However, from a practical point of view, the effectiveness of a seismic early-warning system should be deemed limited. Considering the distances from NE Taiwan to the island's three major metropolitan areas (Taipei, Taichung, and Kaohsiung; Figure 1), the maximum warning time is estimated to be approximately 16.5, 30.5, and 58 s, respectively (Kao *et al.*, 1995). Such a short time constraint is probably barely enough to initiate any disaster-prevention operations.

Last but not the least, it is emphasized once again that proper prevention measures are far more important than anything else when facing potentially devastating threat from earthquakes. Conclusions of the present study can contribute to establish an improved building code and planning of future major industrial facilities in the Taiwan region.

## 6. CONCLUSION

Seismogenic structures in the southernmost Ryukyu arc-Taiwan region are complex. There are four major structures at depths shallower than 70 km: the Collision Seismic Zone (CSZ), the Interface Seismic Zone (ISZ), the Lateral Collision Seismic Zone (LCSZ), and the Okinawa Seismic Zone (OSZ). All of them are capable of generating earthquakes with  $m_b \geq 5.5$ .

The seismogenic conditions along the southernmost Ryukyu interface is addressed in four different aspects. From the historic large and great earthquakes point of view, it is inconclusive whether  $M_w \geq 8$  events did ever occur along the plate interface, but there seems no doubt that at least a few earthquakes with  $M_w \geq 7.0-7.5$  have occurred in the southernmost Ryukyu arc-Taiwan region since the turn of this century. Earthquake focal mechanisms show co-existence of extensional earthquakes in the outer-rise and within the subducted lithosphere, suggesting no patterns of a seismic cycle due to strong coupling along the interface. The lack of "transitional thrust" earthquakes near the lower portion of the seismogenic plate interface further supports that the interface is not strongly coupled. The maximum coherent rupture area for an earthquake occurring along the plate interface is estimated to be on the order of  $3 \times 10^3 \text{ km}^2$  (*i.e.*, 25 km by 120 km), as calculated from the inferred geometric configuration of interface. Assuming a typical value for rigidity and an average amount of dislocation, this faulting area corresponds to a maximum  $M_w$  of 7.6-7.7. The average slip obliquity of interface earthquakes is  $35^\circ$  while the convergence obliquity is  $70^\circ$ . Such a pattern of slip partitioning indicates that the rheological behavior of the Ryukyu fore-arc in this region is not completely elastic, thus is unlikely to generate  $M_w > 8$  subduction earthquakes.

On the other hand, focal mechanisms indicate strong interactions among different tec-

tonic stress regimes, particularly in NE Taiwan. Specifically, most earthquakes showing lateral compressive strain (LCSZ events, Figure 2) also have  $T$ -axes in the extension directions associated with either the Okinawa trough opening or down-dip slab pulling force. Moreover, successive rotation of  $T$ -axes of normal faulting events from N–S within the Okinawa trough to nearly E–W beneath NE Taiwan suggests interactions between the extension and compression associated with the back-arc opening and regional collision, respectively (Kao *et al.*, 1998). Although such interactions may not necessarily mean a bigger event, they are possible to increase the frequency of earthquake occurrence because the combined stress regime would reach the failure criteria of geological materials more effectively. Thus from the seismic hazard point of view, the potential threat from frequent occurrences of  $M_w > 7$  events in the region cannot be ignored.

The existence of a possible tear fault in the region is not conclusive at the moment. The maximum-sized earthquake associated with this structure, assuming it indeed exists, is probably no greater than that along the plate interface. Given that NE Taiwan is the most likely place to have interactions among various stress regimes, it is suggested that seismicity there to be closely monitored. On the other hand, due to the short distances from NE Taiwan to the three largest metropolitan areas on the island, the effect of an early-warning system depending on early detection and fast communication facilities should be deemed limited. Improving and strictly enforcing building code and careful planning of major industrial facilities are probably the best measures when facing potentially devastating threat from earthquakes.

*Acknowledgments* Constructive discussions with Jacques Angelier, Wang-Ping Chen, Ling-Yun Chiao, Shu-Kun Hsu, Jyr-Ching Hu, Serge Lallemand, Jian-Cheng Lee, Char-Shine Liu, Ruey-Juin Rau, Ta-Liang Leon Teng, and Francis T. Wu are greatly appreciated. Thoughtful reviews by Serge Lallemand and two anonymous reviewers significantly improved the manuscript. This research was partially supported by grants from the National Science Council of Taiwan (NSC85-2111-M-001-020-Y) and the Central Weather Bureau (CWB84-2E-22).

## REFERENCES

- Abe, K., 1981: Magnitudes of large shallow earthquakes from 1904 to 1980. *Phys. Earth Planet. Inter.*, **27**, 72–92.
- Aki, K., and P. G. Richards, 1980: Quantitative seismology: Theory and methods, 932 pp., Freeman, San Francisco.
- Allen, C. R., 1962: Circum-Pacific faulting in the Philippine–Taiwan region. *J. Geophys. Res.*, **67**, 4795–4812.
- Astiz, L., and H. Kanamori, 1986: Interplate coupling and temporal variation of mechanisms of intermediate-depth earthquakes in Chile. *Bull. Seismol. Soc. Am.*, **76**, 1614–1622.
- Astiz, L., T. Lay, and H. Kanamori, 1988: Large intermediate-depth earthquakes and the subduction process. *Phys. Earth Planet. Inter.*, **53**, 80–166.
- Beckers, J., and T. Lay, 1995: Very broadband seismic analysis of the 1992 Flores, Indonesia, earthquake ( $M_w = 7.9$ ). *J. Geophys. Res.*, **100**, 18,179–18,193.

- Biq, C.-C., 1972: Dual-trench structure in the Taiwan-Luzon region. *Proc. Geol. Soc. China*, **15**, 66–75.
- Christensen, D. H., and L. J. Ruff, 1983: Outer-rise earthquakes and seismic coupling. *Geophys. Res. Lett.*, **10**, 697–700.
- Christensen, D. H., and L. J. Ruff, 1988: Seismic coupling and outer rise earthquakes. *J. Geophys. Res.*, **93**, 13,421–13,444.
- Delouis, B., T. Monfret, L. Dorbath, M. Pardo, and L. Rivera, 1997: The  $M_w = 8.0$  Antofagasta (Northern Chile) earthquake of 30 July 1995: A precursor to the end of the large 1877 gap. *Bull. Seismol. Soc. Am.*, **87**, 427–445.
- Dmowska, R., J. R. Rice, L. C. Lovison, and D. Josell, 1988: Stress transfer and seismic phenomena in coupled subduction zones during the earthquake cycle. *J. Geophys. Res.*, **93**, 7869–7884.
- Duda, S. J., 1965: Secular seismic energy release in the circum-Pacific belt. *Tectonophysics*, **2**, 409–452.
- Duda, S. J., 1992: Global earthquakes 1903–1985, U.S. Geol. Surv., Open File Rep. 92-360.
- England, P. & G. Houseman, 1989: Extension during continental convergence, with application to the Tibetan Plateau. *J. Geophys. Res.*, **94**, 17,561–17,579.
- Fitch, T. J., 1972: Plate convergence, transcurrent faults, and internal deformation adjacent to southeast Asia and the western Pacific. *J. Geophys. Res.*, **77**, 4432–4460.
- Furukawa, Y., 1993: Depth of the decoupling plate interface and thermal structure under arcs. *J. Geophys. Res.*, **98**, 20,005–20,013.
- Gao, L. & Wallace, T. C., 1995. The 1990 Rudbar-Tarom Iranian earthquake sequence: Evidence for slip partitioning, *J. Geophys. Res.*, **100**, 15,317–15,332.
- Geller, R. J. & Kanamori, H., 1977. Magnitudes of great shallow earthquakes from 1904 to 1952, *Bull. Seismol. Soc. Am.*, **67**, 587–598.
- Ghose, S., Mellors, R. J., Korjenkov, A. M., Hamburger, M. W., Pavlis, T. L., Pavlis, G. L., Omuraliev, M., E. Mamyrov, and A. R. Muraliev, 1997: The  $M_s = 7.3$  1992 Suusamy, Kyrgyzstan, earthquake in the Tien Shan: 2. Aftershock focal mechanisms and surface deformation. *Bull. Seismol. Soc. Am.*, **87**, 23–38.
- Gutenberg, B., and C. F. Richter, 1954: Seismicity of the Earth, 2nd ed., 330 pp., Princeton University Press, Princeton, N.J.
- Ho, C. S., 1988: An introduction to the geology of Taiwan, 2nd, 192 pp., Central Geological Survey, The Ministry of Economic Affairs, Taipei.
- Hu, J.-C., and J. Angelier, 1996: Modeling of stress-deformation relationships in a collision belt: Taiwan. *TAO*, **7**, 447–465.
- Imanishi, M., F. Kimata, N. Inamori, R. Miyajima, and Hirahara K., 1996: Horizontal displacements by GPS measurements at the Okinawa–Sakishima Islands (in Japanese). *J. Seismol. Soc. Jpn.*, **49**, 417–421.
- Isacks, B., and P. Molnar, 1969: Mantle earthquake mechanisms and the sinking of the lithosphere. *Nature*, **233**, 1121–1124.
- Isacks, B., and P. Molnar, 1971: Distribution of stresses in the descending lithosphere from a global survey of focal-mechanism solutions of mantle earthquakes. *Rev. Geophys.*, **9**,

103–174.

- Jarrard, R. D., 1986: Relations among subduction parameters. *Rev. Geophys.*, **24**, 217–284.
- Kagan, Y. Y., and D. D. Jackson, 1994: Long-term probabilistic forecasting of earthquakes. *J. Geophys. Res.*, **99**, 13,685–13,700.
- Kanamori, H., 1970: The Alaska earthquake of 1964: Radiation of long-period surface waves and source mechanism. *J. Geophys. Res.*, **75**, 5029–5040.
- Kanamori, H., 1977: Seismic and aseismic slip along subduction zones and their tectonic implications in Island Arcs, Deep Sea Trenches and Back-Arc Basins, Maurice Ewing Ser., M. Talwani & W. C. Pitman, III ed.
- Kanamori, H., 1978: Quantification of earthquakes. *Nature*, **271**, 411–414.
- Kao, H., and W.-P. Chen, 1991: Earthquakes along the Ryukyu–Kyushu arc: Strain segmentation, lateral compression, and the thermomechanical state of the plate interface. *J. Geophys. Res.*, **96**, 21,443–21,485.
- Kao, H., and W.-P. Chen, 1995: Transition from interplate slip to double seismic zone along the Kuril–Kamchatka arc. *J. Geophys. Res.*, **100**, 9881–9903.
- Kao, H., and W.-P. Chen, 1996: Seismicity in the outer-rise–forearc region and configuration of the subducting lithosphere with special reference to the Japan trench. *J. Geophys. Res.*, **101**, 27,811–27,831.
- Kao, H., S. J. Shen, T.-C. Shin, and Z.-S. Tsai, 1995: Planning of an early-warning system for seismogenic structures along the subduction zone beneath NE Taiwan, in Central Weather Bureau Res. Rep. 450, pp. 185–218.
- Kao, H., S. J. Shen, and K.-F. Ma, 1998: Transition from oblique subduction to collision: Earthquakes in the southernmost Ryukyu arc–Taiwan region. *J. Geophys. Res.*, in press.
- Kelleher, J., L. Sykes, and J. Oliver, 1973: Possible criteria for predicting earthquake locations and their application to major plate boundaries of the Pacific and the Caribbean. *J. Geophys. Res.*, **78**, 2547–2585.
- Kelleher, J., J. Savino, H. Rowlett, and W. McCann, 1974: Why and where great thrust earthquakes occur along island arcs. *J. Geophys. Res.*, **79**, 4889–4899.
- Lallemand, S. E., C.-S. Liu, and Y. Font, 1997: A tear fault boundary between the Taiwan orogen and the Ryukyu subduction zone. *Tectonophysics*, **274**, 171–190.
- Lay, T., L. Astiz, H. Kanamori, and D. H. Christensen, 1989: Temporal variation of large intraplate earthquakes in coupled subduction zones. *Phys. Earth Planet. Inter.*, **54**, 258–312.
- Liu, C.-C., 1995: The Ilan plain and the southwestward extending Okinawa trough. *J. Geol. Soc. China*, **38**, 229–242.
- Liu, X., K. C. McNally, and Z.-K. Shen, 1995: Evidence for a role of the downgoing slab in earthquake slip partitioning at oblique subduction zones. *J. Geophys. Res.*, **100**, 15,351–15,372.
- McCaffrey, R., 1992: Oblique plate convergence, slip vectors, and forearc deformation. *J. Geophys. Res.*, **97**, 8905–8915.
- McCaffrey, R., 1993: On the role of the upper plate in great subduction zone earthquakes. *J. Geophys. Res.*, **98**, 11,953–11,966.

- McCaffrey, R., 1994: Global variability in subduction thrust zone-Forearc systems. *Pure Appl. Geophys.*, **142**, 173–224.
- McCaffrey, R., 1996: Estimates of modern arc-parallel strain rates in fore arcs. *Geology*, **24**, 27–30.
- Mellors, R. J., F. L. Vernon, G. L. Pavlis, G. A. Abers, M. W. Hamburger, S. Ghose, and B. Iliasov, 1997: The Ms = 7.3 1992 Suusamy, Kyrgyzstan, earthquake: 1. Constraints on fault geometry and source parameters based on aftershocks and body-wave modeling. *Bull. Seismol. Soc. Am.*, **87**, 11–22.
- Nishenko, S. P., and K. H. Jacob, 1990: Seismic potential of the Queen Charlotte-Alaska-Aleutian seismic zone. *J. Geophys. Res.*, **95**, 2511–2532.
- Pacheco, J. F., and L. R. Sykes, 1992: Seismic moment catalog of large, shallow earthquakes, 1900–1989. *Bull. Seismol. Soc. Am.*, **82**, 1306–1349.
- Pacheco, J. F., L. R. Sykes, and C. H. Scholz, 1993: Nature of seismic coupling along simple plate boundaries of the subduction type. *J. Geophys. Res.*, **98**, 14,133–14,159.
- Rau, R.-J., and F. T. Wu, 1995: Tomographic imaging of lithospheric structures under Taiwan. *Earth Planet. Sci. Lett.*, **133**, 517–532.
- Richter, C. F., 1958: *Elementary Seismology*, 712 pp., Freeman, San Francisco, Calif.
- Ruff, L. J., 1989: Do trench sediments affect great earthquake occurrence in subduction zones?. *Pure Appl. Geophys.*, **129**, 263–282.
- Ruff, L. J., and H. Kanamori, 1983: Seismic coupling and uncoupling at subduction zones. *Tectonophysics*, **99**, 99–117.
- Sato, T., S. Koresawa, Y. Shiozu, F. Kusano, S. Uechi, O. Nagaoka, and J. Kasahara, 1994: Microseismicity of back-arc rifting in the middle Okinawa Trough. *Geophys. Res. Lett.*, **21**, 13–16.
- Scholz, C. H., and J. Campos, 1995: On the mechanism of seismic decoupling and back arc spreading at subduction zones. *J. Geophys. Res.*, **100**, 22,103–22,115.
- Seno, T., S. Stein, and A. E. Gripp, 1993: A model for the motion of the Philippine Sea Plate consistent with NUVEL-1 and geological data. *J. Geophys. Res.*, **98**, 17,941–17,948.
- Sibuet, J.-C., J. Letouzey, F. Barbier, J. Charvet, J.-P. Foucher, T. W. C. Hilde, M. Kimura, C. Ling-Yun, B. Marsset, C. Muller, and J.-F. Stephan, 1987: Back arc extension in the Okinawa trough. *J. Geophys. Res.*, **92**, 14,041–14,063.
- Suárez, G., and O. Sánchez, 1996: Shallow depth of seismogenic coupling in southern Mexico: Implications for the maximum size of earthquakes in the subduction zone. *Phys. Earth Planet. Inter.*, **93**, 53–61.
- Tichelaar, B. W., and L. J. Ruff, 1991: Seismic coupling along the Chilean subduction zone. *J. Geophys. Res.*, **96**, 11,997–12,022.
- Tsai, Y.-B., 1986: Seismotectonics of Taiwan. *Tectonophysics*, **125**, 17–37.
- Usami, T., 1981: Worldwide earthquake catalog, 1900–1962. *World Data Center A for Solid Earth Geophys.*, **Rep. SE-28**, 40–67.
- Velasco, A. A., C. J. Ammon, T. Lay, and M. Hagerty, 1996: Rupture process of the 1990 Luzon, Philippines ( $M_w=7.7$ ), earthquake. *J. Geophys. Res.*, **101**, 22,419–22,434.
- Wu, F. T., 1978: Recent tectonics of Taiwan. *J. Phys. Earth*, **26 (suppl.)**, S265–S299.

- Yeh, Y.-H., C.-H. Lin, and S. W. Roecker, 1989: A study of upper crustal structures beneath northeastern Taiwan: Possible evidence of the western extension of Okinawa trough. *Proc. Geol. Soc. China*, **32**, 139–156.